2011

A reactive wet spinning approach to polypyrrole fibres

Javad Foroughi
University of Wollongong, foroughi@uow.edu.au

Geoffrey M. Spinks
University of Wollongong, gspinks@uow.edu.au

G G. Wallace
University of Wollongong, gwallace@uow.edu.au

Journal of Materials Chemistry

Cite this: *J. Mater. Chem.*, 2011, **21**, 6421

www.rsc.org/materials

PAPER

A reactive wet spinning approach to polypyrrole fibres

Javad Foroughi, Geoffrey M. Spinks and Gordon G. Wallace*

Received 16th December 2010, Accepted 15th February 2011
DOI: 10.1039/c0jm04406g

Electrically conducting, robust fibres comprised of both an alginate (Alg) biopolymer and a polypyrrole (PPy) component have been produced using reactive wet-spinning. Using this approach polypyrrole–biopolymer fibres were also produced with single-walled carbon nanotubes (CNTs), added to provide additional strength and conductivity. SEM images of the PPy–Alg composite fibres clearly show the tubular multifilament form of the alginate fibre impregnated with PPy nanoparticles. The fibres produced containing CNTs show a 78% increase in ultimate stress and 25% increase in elongation to break compared to PPy–alginate fibre. Young's modulus obtained for the PPy–Alg–CNT fibres showed a 30% increase compared to the PPy–alginate fibre. The fibres produced were electrochemically active and capable of electromechanical actuation with a strain of 0.7% produced at a scan rate of 100 mV s^{-1} of the potential.

1. Introduction

Conducting and biocompatible polymer fibres are likely to be important for *in vivo* bioengineering applications, as they allow the incorporation of desirable features such as chemical or biochemical triggers (drugs, growth factors), changing mechanical properties on demand, or even electrically induced movement or force generation. Polypyrrole (PPy) is a well known conducting polymer that has been used in a range of applications including biosensors[1] as platforms for mammalian cell growth,[2,3] battery electrodes, gas sensors, biological sensors, ion-sieving, corrosion protection, microwave shielding, e-textiles and artificial muscle.[4–18] However, PPy manufactured by conventional chemical and electrochemical methods is normally insoluble in common organic solvents,[19] a feature attributed to the presence of strong interchain interactions.[19,20]

As a consequence of low solubility, PPy films are normally prepared electrochemically with the size of the film restricted by the electrode substrate area employed. Continuous production of conducting polymer fibres based on polypyrrole has been limited due to a lack of solubility. A wet-spinning process[21,22] utilising a very specific dopant di-(2-ethylhexyl) sulfosuccinate (DEHS) to induce solubility in the PPy material has been described. However, since the properties of PPy are greatly influenced by the choice of dopant, it is desirable to develop a fibre spinning process that enables a wider range of dopants to be incorporated.

The use of a reactive spinning process wherein a host fibre containing a monomer is subsequently exposed to an oxidant to induce conducting polymer formation is a possible route to achieving PPy containing fibres. Given our ultimate goal is to apply these fibres in biological applications, the use of suitable biopolymers as the host structure for the pyrrole monomer appears to be an attractive approach.

Alginate (Alg), which is obtained from marine brown algae, is a water-soluble polymer and gels in the presence of certain divalent cations such as Ca^{2+}. Alginate fibres have been produced by wet-spinning and found to be non-toxic, biocompatible and biodegradable.[23,24] Here we explore the use of alginate as a host fibre containing pyrrole monomer which is subsequently converted to the conducting polymer. In a further aspect of the work, we have investigated the use of carbon nanotubes (CNTs) to provide mechanical reinforcement and to bolster conductivity; as has been reported previously for conducting polymer fibres[25] and for non-conducting polymers including alginate.[26]

The present work, considers the properties of doped PPy–alginate conducting fibres with and without CNTs present. The preparation method allows different dopants to be used with the PPy, and herein we compare the properties of PPy–Alg fibres with two different dopants.

2. Experimental

2.1. Materials

Di-(2-ethylhexyl) sulfosuccinate sodium salt (Na^+DEHS^-), ammonium peroxydisulfate (APS), sodium *p*-toluenesulfonate (*p*TS), ferric chloride, Triton-X100, and calcium chloride were supplied by Sigma-Aldrich and used as received. Sodium alginate ($M_W \approx 400\,000$ Da) was purchased from Kibun Food Chemifer (China). Pyrrole monomer (95%, Aldrich) was used after distillation. Purified single-walled carbon nanotubes (SWNTs) obtained from Carbon Nanotechnologies Incorporated (CNI,

ARC Centre of Excellence for Electromaterials Science, Intelligent Polymer Research Institute, University of Wollongong, Northfields Avenue, Wollongong, NSW, 2522, Australia. E-mail: gwallace@uow.edu.au; Fax: +61 2 42213114; Tel: +61 2 42213127

USA) were used without treatment and contained 5 wt% iron residue as determined by elemental analysis.

2.2. Preparation of spinning solution

To prepare PPy–Alg fibres, a spinning solution was prepared in the following manner: 3.2 g of pyrrole were added to 60 ml alginate solution (2% w/v) and stirred for 1 h. To improve miscibility of the solution, 0.1% (w/v) of DEHS as a surfactant was added to the previously prepared solution. The weight ratio of pyrrole monomer to alginate polymer in this spinning solution was 2.66 : 1. To produce PPy–Alg–CNTs composite fibres, 64 mg of single-walled carbon nanotubes were sonicated for 1 h in 80 ml water containing 0.1% w/w Triton-X100. Then 1.6 g of alginate powder were added into the SWNT dispersion and the solution was stirred for 24 h. Next, 4.2 g of pyrrole were added into the alginate–CNT dispersion with further stirring for 1 h. The final weight ratio of pyrrole monomer to alginate to SWNT was 2.63 : 1 : 0.04.

2.3. Fibre spinning

Fibre spinning was carried out using a continuous *in situ* wet-spinning and polymerization process (Fig. 1). Prior to spinning, the solution was passed through a 200 μm filter using a nitrogen pressure vessel. The filtered solution was transferred to a syringe and a syringe pump was used to drive the spinning solution through a single hole spinneret with $D = 100$ μm and finally into the coagulation bath. The coagulation bath contained a 5% w/v solution of $CaCl_2$ in a mixture of methanol/water (70/30) solvent. The syringe pump flow rate was adjusted to 50 ml h^{-1} to control the injection rate for the reactive spinning dopes to control the fibre formation process. The as-spun fibres were drawn to 7.5 times during wet spinning and continuously passed through an oxidant/dopant bath containing an [oxidant]/[dopant] ratio of 1.3 (concentration of oxidant 3 wt%). The following oxidant/dopant systems were employed: APS/DEHS; APS/*p*TS; $FeCl_3$/DEHS or $FeCl_3$/*p*TS in 30 ml water. The pyrrole monomer retained in the coagulated fibre is polymerized in this second bath. In the case of PPy–alginate fibre, the colour changed from white to black/green after a few minutes, demonstrating the formation of PPy. The nascent fibres were collected on the drum and then kept in air for 2 h. Post-spinning treatment was carried out using a bath containing a 15% w/v solution of $CaCl_2$ in a mixture of methanol/water (70/30) solvent at 20 °C for 1.5 h. As-spun PPy–Alg–CNT fibres prepared as above are referred to hereafter as PPy–Alg–CNT (APS/DEHS); PPy–Alg–CNT (APS/*p*TS), PPy–Alg–CNT ($FeCl_3$/*p*TS) and PPy–Alg–CNT ($FeCl_3$/DEHS) to emphasize the different oxidant/dopant systems used. The properties of PPy–Alg and PPy–Alg–CNT fibres were compared with bare alginate fibres produced from neat alginate solution (2% v/v).

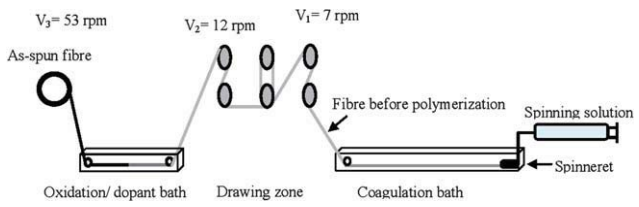

Fig. 1 Continuous wet-spinning and polymerization line.

2.4. Instrumentation

A Leica Stereoscan 440 scanning electron microscope (SEM) was employed for morphological studies. Fibre samples were fractured after cooling in liquid N_2 to obtain circular undamaged cross-sections. Small pieces of fibre were fixed vertically on an aluminium stub using conductive glue. A sputter coater (Dynavac) was used for coating of a thin layer of gold on the cross-section and side wall of the fibres under sputtering conditions of 45 mA for 12 s under 200 mbar of inert argon gas.

Tensile testing was carried out using a dynamic mechanical analyser (TA instrument, USA). A 10 mm gauge length of fibre was stretched at a strain rate of 500 μm min^{-1} at 25 °C until the sample broke or yielded. To obtain accurate results for mechanical properties, 3 samples were tested from each fibre type.

UV-Vis/NIR spectra were obtained using a Cary 5000 spectrophotometer.

A three electrode electrochemical cylindrical cell (15 × 50 mm) coupled to a Bioanalytical Systems (Model CV27) potentiostat was used for cyclic voltammetry. A 10 mm fibre was used as the working electrode with an Ag/AgCl reference electrode and a Pt mesh counter electrode. The electrolyte was 1 M $NaNO_3$.

The viscosity of spinning solution was recorded with an Anton Paar viscometer (physical MCR 301) using Rheoplus software.

Electrochemical actuation studies of fibres were carried out using a three-electrode system including a reference electrode. The working electrode was the PPy–Alg–CNT fibre and the auxiliary electrode was a piece of Pt mesh. Ag/AgCl in 3 M NaCl was used as reference electrode. A dual mode lever arm system (Auroa Scientific Inc) was used for the actuation tests. The sample extension/contraction was measured by the arm on which the sample was attached. The device is able to work in both mechanical modes: isotonic (control force, measure displacement) and isometric (control displacement, measure force).

Optical microscopy (Nikon TE 300/2000) was employed to determine diameter and cross-section area of fibres.

3. Results and discussion

Solutions to be used for fibre spinning were prepared as described in the Experimental section. In all cases agglomerate free systems were obtained.

3.1. Viscometry of spinning solution

The complex viscosity for each of the solutions was obtained as a function of shear rate (Fig. 2). It was found that the addition of pyrrole to the alginate solution had minimal effect on the viscosity. Moreover, the addition of CNTs had no significant effect on the spinning. The viscosity slightly decreased at higher shear rates due to the presence of the surfactant (Triton-X100) in the added CNT dispersion. For continuous fibre spinning, high shear rates occur at the orifice of the spinneret, so viscosity at these conditions can influence the spinning process. The small variations in viscosity shown in Fig. 2 did not influence the spinnability of the three compositions.

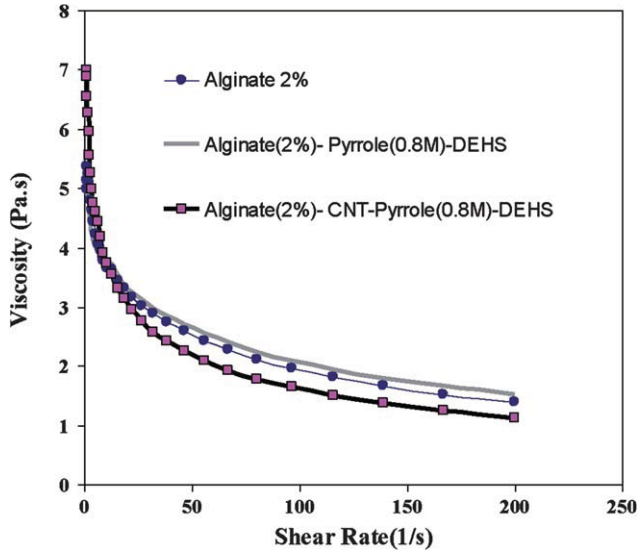

Fig. 2 Variation in viscosity at different shear rates of spinning solutions of alginate and alginate–pyrrole with and without CNTs.

3.2. Fibre spinning

As-spun fibres were characterized during and after fibre spinning to optimize spinning conditions. Both the PPy–Alg and PPy–CNT–Alg fibres were spun at same condition of wet-spinning process.

3.3. UV-Vis/NIR spectroscopy of as-spun fibre

In the case of the fibres containing pyrrole an obvious darkening of the fibre, indicative of polypyrrole formation, was observed after passing through the oxidant bath. To quantify polymer growth, UV-Vis/NIR spectra of as-spun PPy–DEHS/Alg were measured in the range 300–1100 nm before entering the oxidation bath (*i.e.* time = 0) and at various times after leaving the bath. As can be seen from Fig. 3, two peaks (~450 nm and 800–950 nm) were observed after the fibre had passed through the oxidant bath. Previous reports [21,22] show that polypyrrole displays strong absorption peaks at ~450 nm (assigned to transitions from the PPy valence band to an antibonding-bipolaron band) as well as intense, broad absorptions covering the NIR region, with maxima at 970 nm. This NIR absorption is attributed to electron transitions from the polypyrrole valence band to a second bipolaron band in the band gap.[27] The appearance of peaks at ~450 nm and 800–950 nm in the fibres confirms the formation of conductive polypyrrole. The intensity of these peaks steadily increased over the first 45 minutes after contact with the oxidant bath, indicating an increase in PPy concentration within the fibres. No further PPy formation was obvious after 45 minutes. Although it was not possible to conduct the UV-Vis/NIR analysis when CNTs were present (due to the strong absorbance by CNTs) it was assumed that the PPy formation proceeded at a similar rate.

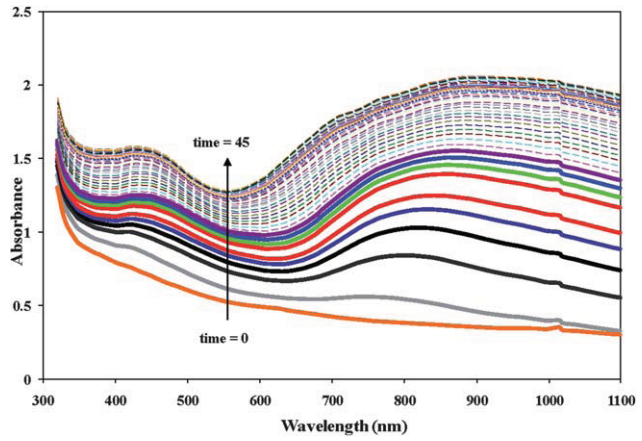

Fig. 3 UV-Vis/NIR spectra of as-spun alginate–pyrrole fibre. Time = 0 is the point at which the alginate–pyrrole fibre enters the oxidation bath from the drawing zone (see Fig. 1). Time = 45 is 45 min after the fibre had first contact with the oxidant bath.

3.4. Morphology of as-spun fibres

SEM micrographs of alginate, PPy–Alg and PPy–Alg–CNT fibres were obtained (Fig. 4). While the surface of the Alg fibres was quite smooth (Fig. 4a), all fibres containing PPy showed a rough surface (Fig. 4b–d) and non-uniform cross-sectional shape (Fig. 4e). The rough surface of PPy–Alg fibres can be clearly seen at higher magnification in Fig. 4d. The surface has a similar appearance to electrochemically deposited PPy on various substrates described previously.[28] While CNTs are clearly observed on the cross-sectional micrograph of PPy–Alg–CNT fibres (Fig. 4f), the CNTs cannot be observed on the surface.

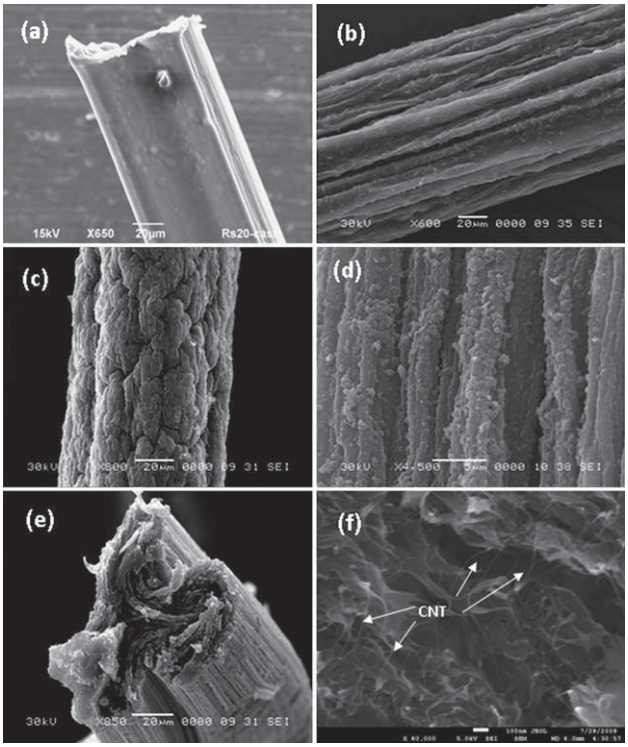

Fig. 4 SEM micrographs of the fibres: surface (a) alginate, (b) PPy–(APS/DEHS)–Alg, (c) PPy–(APS/DEHS)–Alg–CNT and (d) higher magnification PPy–(APS/DEHS)–Alg, cross-sectional: (e) PPy–(APS/DEHS)–Alg, (f) PPy–(APS/DEHS)–Alg–CNT.

Surface and cross-section morphology of the PPy–Alg–CNT nanocomposite fibres at high magnification and prepared with different oxidant/dopant systems are shown in Fig. 5. Only minor differences in morphology were observed in the fibres, suggesting that the oxidant/dopant used does not significantly alter the fibre microstructures. CNTs were observed in the cross-sectional images of all fibres (Fig. 5b,d and f), regardless of the oxidant/dopant used.

3.5. Mechanical properties of as-spun PPy–Alg and PPy–Alg–CNT fibres

The mechanical, thermal, electrical and electrochemical properties of the fibres were also determined. Fig. 6 shows mechanical properties of Alg, PPy–Alg fibres, and PPy–Alg–CNT nanocomposite fibre where APS/DEHS was used as oxidant/dopant for pyrrole polymerisation. Ultimate stresses of ~307 ± 10 MPa, ~140 ± 6 MPa and ~250 ± 5 MPa with ~12 ± 2% strain, ~8 ± 1.5% strain and ~10 ± 1.3% strain were obtained for the alginate, PPy–Alg and PPy–Alg–CNT fibres, respectively. Similarly, Young's moduli were found to be 13 ± 2, 7 ± 1, and 10 ± 0.5 GPa for the alginate, PPy–Alg and PPy–Alg–CNT fibres, respectively. These results confirm the reinforcing role played by CNTs in the PPy–Alg fibres. However, the decrease in mechanical properties of the alginate fibre with the addition of PPy (with or without CNTs) was unexpected and may be due to the low compatibility of alginate and PPy. Phase separation of the hydrophilic alginate and hydrophobic PPy may introduce stress-concentration at the phase interface that would lower the tensile strength and elongation at break. The modulus also could be reduced by low adhesion at the interface. Bicomponent polyaniline (PAni)-nylon fibres showed a similar reduction in nylon mechanical properties through the addition of PAni.[29]

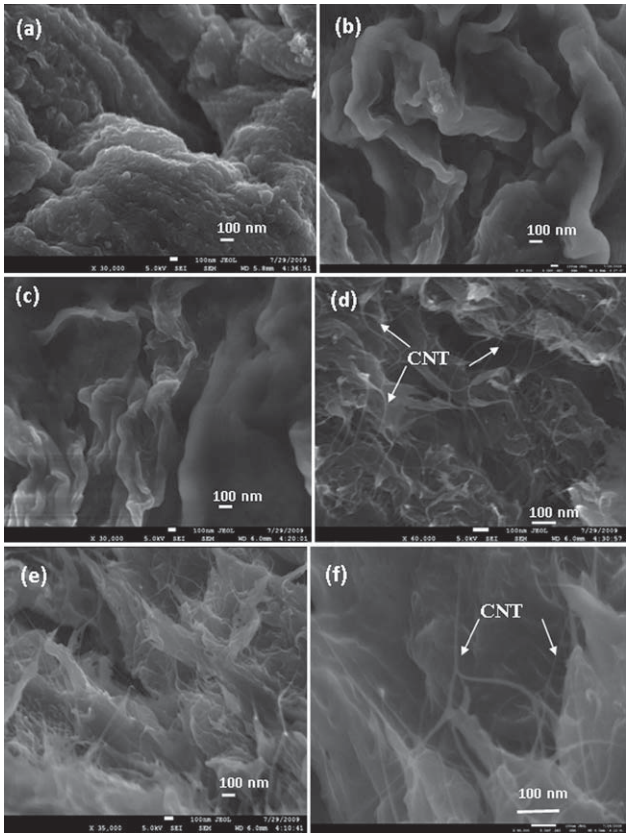

Fig. 5 SEM micrographs at high magnification of the as-spun PPy–Alg–CNT fibres with different oxidant/dopant systems: surface (a) APS/*p*TS, (b) $FeCl_3$/DEHS, (c) $FeCl_3$/*p*TS and cross-sectional: (d) APS/*p*TS, (e) $FeCl_3$/DEHS, (f) $FeCl_3$/*p*TS.

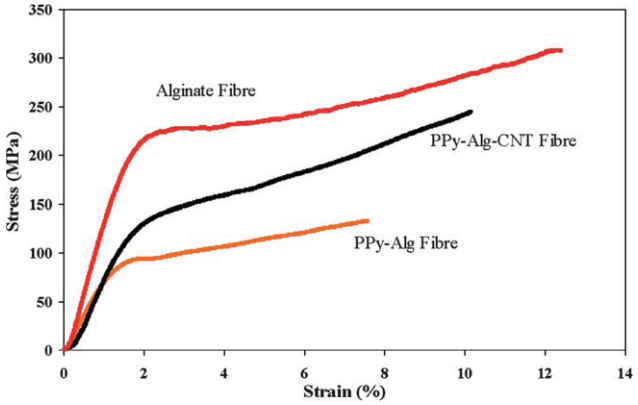

Fig. 6 Stress–strain curves obtained from tensile tests of alginate fibre, PPy–Alg and PPy–Alg–CNT composite fibres. APS/DEHS was used as oxidant/dopant for the pyrrole polymerisation in each case.

The effect of dopant and oxidant on the mechanical properties of PPy–Alg–CNT nanocomposite fibres was also investigated. A comparison of the stress–strain curves for the various prepared fibres is given in Fig. 7. When APS was used as oxidant, a similar tensile strength was observed for both *p*TS and DEHS dopants. However, a smaller strain at break of 5% was obtained in the *p*TS doped polymer compared with 10% in the DEHS PPy. The use of ferric chloride as oxidant produced fibres with significantly lower Young's modulus and tensile strength compared with the APS polymerised pyrrole. Tensile stresses of 95 ± 4 MPa and 65 ± 8 MPa with ~5 ± 1% strain and 4 ± 0.7% strain were obtained for PPy–Alg–CNT ($FeCl_3$/DEHS) and PPy–Alg–CNT ($FeCl_3$/*p*TS), respectively. Young's modulus was measured to be 11.8 ± 2 and 3.7 ± 0.8 GPa for APS/*p*TS and $FeCl_3$/*p*TS, respectively. These results show that APS is the preferred oxidant for reactive spinning of PPy fibres.

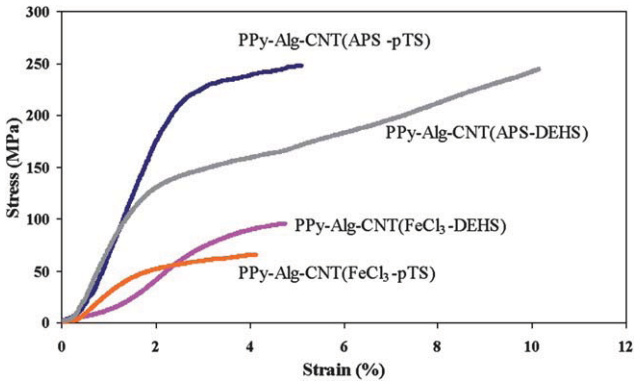

Fig. 7 Stress–strain curves obtained from tensile tests of PPy–Alg–CNT nanocomposite fibres with different oxidant/dopant systems.

Table 1 Effect of the oxidant/dopant on electrical conductivity of as-spun fibres

Material	Conductivity/S cm^{-1}
PPy–Alg (APS/DEHS)	0.5 ± 0.2
PPy–Alg–CNT (APS/DEHS)	3.0 ± 0.5
PPy–Alg–CNT ($FeCl_3$/DEHS)	2.0 ± 0.4
PPy–Alg–CNT (APS/*p*TS)	4.0 ± 0.8
PPy–Alg–CNT ($FeCl_3$/*p*TS)	10.0 ± 1.5

Upon immersion in water, a swelling ratio of ~200% was observed for PPy–Alg fibres. However, the swelling ratio observed for PPy–Alg–CNT (APS/DEHS) fibres was reduced significantly to 50%, while it was found to be 170% for bare alginate fibres. These results suggest that CNTs can act as reinforcement agents between alginate microfibres.

3.6. Electrical and electrochemical properties of as-spun fibres

The average electrical conductivity of PPy–Alg fibre was measured to be ~0.5 S cm^{-1} which was increased to 3 S cm^{-1} by the addition of CNTs. Use of other oxidant and dopant systems affected the conductivity, with the highest value (10 S cm^{-1}) obtained using $FeCl_3$ and *p*TS (Table 1). All these conductivity values were considerably lower than the electrical conductivity of wet-spun PPy–DEHS,[1,2] which is likely due to the presence of non-conductive alginate polymer.

Drawn PPy fibres from high molecular weight PPy–DEHS[22] show an electrical conductivity of 30 S cm^{-1} which is three times higher than best value of PPy–Alg–CNT ($FeCl_3$/*p*TS) fibres (10 S cm^{-1}). However, PPy fibres from low molecular weight PPy–DEHS[21] show an electrical conductivity of 3 S cm^{-1} which is almost similar to PPy–Alg–CNT fibres and it is slightly higher than PPy–Alg fibres. The small differences that occur using the different dopants may arise from slightly different morphologies in the PPy–Alg–CNT fibres.

Cyclic voltammograms for the PPy–Alg and PPy–Alg–CNT fibres in 1.0 M $NaNO_3$ are shown in Fig. 8. Each exhibited reasonable electroactivity, as evidenced by redox peaks at −0.2 to +0.1 V (PPy–Alg fibre) and −0.4 to 0 V (PPy–Alg–CNT fibre) *vs.* Ag/AgCl reference electrode, respectively. The redox activity in these fibres occurs at different potentials to those previously reported for chemically prepared PPy–DEHS fibre.[2,3] These differences in redox potentials probably reflect the influence of the two different polymers incorporated as well as possible differences in molecular weight, crosslinking and molecular order of the polymers.

Electrochemical actuation of the PPy–Alg–CNT nanocomposite fibre was also examined in an electrolyte composed of 0.1 M DEHS dissolved in acetonitrile–water (1 : 1) (Fig. 9). The nanocomposite gave a reversible actuation strain of ~0.7% at high scan rate (100 mV s^{-1}). The smaller actuation in the PPy–Alg–CNT fibre is probably due to the lower PPy content and the phase separation structure, with the active PPy dispersed throughout the inactive alginate matrix. PPy–Alg fibres were not useable as actuators because of their poor mechanical properties in the wet state.

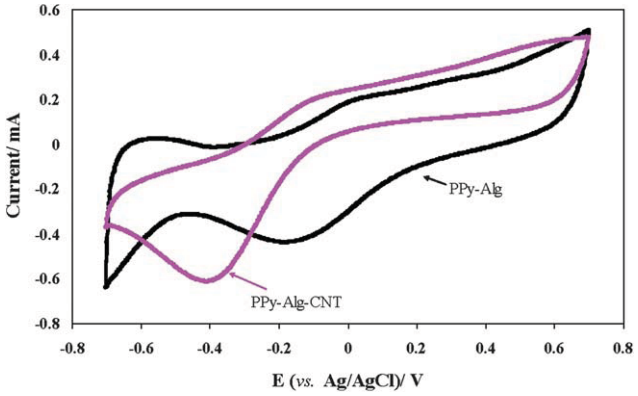

Fig. 8 Cyclic voltammograms of PPy–Alg and PPy–Alg–CNT (APS/DEHS) fibres. Potential was scanned between −0.7 and +0.7V (*vs.* Ag/AgCl) in 1.0 M $NaNO_3$ at 100 mV s^{-1}.

4. Conclusions

Composite fibres of PPy–alginate with and without the inclusion of CNTs were produced using a reactive spinning procedure. Pyrrole monomer was incorporated into alginate or Alg–CNT fibres, and then exposed to various oxidants/dopants to produce PPy. The mechanical properties of PPy–Alg and PPy–Alg–CNT fibres were significantly enhanced compared to the PPy fibre.[21,22] PPy–Alg fibres and PPy–Alg–CNT nanocomposite fibres, exhibited breaking stresses of ~140 and ~250 MPa with ~8% strain and ~10% strain, respectively. Similarly, Young's modulus of PPy–Alg fibres was 7 GPa, compared to 10 GPa for PPy–Alg–CNT nanocomposite fibres. The potential applications of the novel multicomponent biofibres have been evaluated using cyclic voltammetry and actuation tests.

The PPy–Alg–CNT nanocomposite fibres were prepared using various oxidant/dopant systems in the reactive spinning process. The use of ferric chloride as oxidant had a significant influence on the mechanical properties of the fibre produced, with the fibre strength dramatically decreasing compared to fibres produced with APS as oxidant. However, the use of $FeCl_3$/*p*TS as oxidant/dopant in the reactive spinning of PPy–Alg–CNT nanocomposite fibres gave an electrical conductivity that was significantly higher. PPy–Alg–CNT nanocomposite fibres showed reasonable

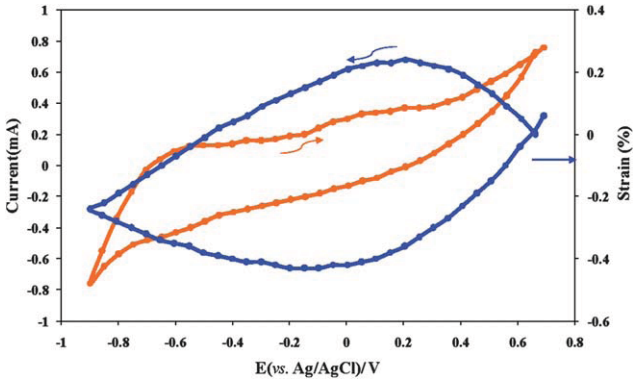

Fig. 9 Cyclic voltammograms of PPy–Alg–CNT (APS/DEHS) fibre. Potential was scanned between −0.9V and +0.7V (*vs.* Ag/AgCl) in 0.1 M DEHS in acetonitrile–water (1 : 1) at 100 mV s^{-1}. (Cycle direction is shown by arrows.)

electroactivity. The results obtained suggest that the electrically conducting PPy containing biofibres produced here may be useful as sensors, actuators, and in some biomedical applications.

Acknowledgements

The authors gratefully acknowledge the financial support of the Australian Research Council.

References

1 R. E. Ionescu, K. Abu-Rabeah, S. Cosnier and R. S. Marks, *Electrochem. Commun.*, 2005, **7**(12), 1277–1282.
2 M. J. Razal, M. Kita, F. A. Quigley, E. Kennedy, E. S. Moulton, M. I. R. Kapsa, M. G. Clark and G. G. Wallace, *Adv. Funct. Mater.*, 2009, **19**(21), 3381–3388.
3 F. A. Quigley, M. J. Razal, C. B. Thompson, E. S. Moulton, M. Kita, L. E. Kennedy, M. G. Clark, G. G. Wallace and M. I. R. Kapsa, *Adv. Mater.*, 2009, **21**(43), 4393.
4 Y. Bar-Cohen, *Electroactive Polymer [EAP] Actuators as Artificial Muscles*, SPIE, The International Society for Optical Engineering, USA, 2nd edn, 2004.
5 P. Hacarlioglu, L. Toppare and L. Yilmaz, *J. Membr. Sci.*, 2003, **225**(1–2), 51.
6 H. Eva, K. Akif, L. Tong, N. Saeid, J. Trevor and H. Eric, *Synth. Met.*, 2004, **144**(1), 21.
7 S. Hara, T. Zama, W. Takashima and K. Kaneto, *J. Mater. Chem.*, 2004, **14**(10), 1516.
8 S. Hara, T. Zama, W. Takashima and K. Kaneto, *Synth. Met.*, 2006, **156**(2–4), 351.
9 J. H. Kim, A. K. Sharma and Y. S. Lee, *Mater. Lett.*, 2006, **60**(13–14), 1697.
10 M. S. Kim, H. K. Kim, S. W. Byun, S. H. Jeong, Y. K. Hong, J. S. Joo, K. T. Song, J. K. Kim, C. J. Lee and J. Y. Lee, *Synth. Met.*, 2002, **126**(2–3), 233.
11 K. Nilgun, O. N. Koken, U. Belkis and A. Ahmet, *Eur. Polym. J.*, 2006, **42**(10), 2361.
12 T. F. Otero and M. T. Cortes, *Chem. Commun. (Cambridge, UK)*, 2004, 284.
13 P. Novak and W. Vielstich, *J. Electrochem. Soc.*, 1990, **137**(4), 1036–1041.
14 S. Walkiewicz, A. Michalska and K. Maksymiuk, *Electroanalysis*, 2005, **17**(14), 1269.
15 O. Yavuz, M. K. Ram, M. Aldissi, P. Poddar and H. Srikanth, *Synth. Met.*, 2005, **151**(3), 211.
16 T. Zama, S. Hara, W. Takashima and K. Kaneto, *Jpn. J. Appl. Phys., Part 1*, 2005, **44**(11), 8153.
17 J. Foroughi, S. R. Ghorbani, G. Peleckis, G. M. Spinks, G. G. Wallace, X. L. Wang and S. X. Dou, *J. Appl. Phys.*, 2010, **107**, 103712–103714.
18 J. Foroughi, G. M. Spinks, G. G. Wallace, *Sens. Actuators, B*, in press.
19 A. Bhattacharya and A. De, *J. Macromol. Sci., Rev. Macromol. Chem. Phys.*, 1999, **39**, 17–56.
20 E. C. Chang, M. Y. Hua and S. A. Chen, *J. Polym. Res.*, 1998, **5**, 249–254.
21 J. Foroughi, G. M. Spinks, G. G. Wallace and P. G. Whitten, *Synth. Met.*, 2008, **158**(3–4), 104–107.
22 J. Foroughi, G. M. Spinks and G. G. Wallace, *Synth. Met.*, 2009, **159**(17–18), 1837–1843.
23 C. J. Knill, J. F. Kennedy, J. Mistry, M. Miraftab, G. Smart, M. R. Groocock and H. J. Williams, *Carbohydr. Polym.*, 2004, **55**(1), 65–76.
24 Y. Qin, *Polym. Int.*, 2008, **57**(2), 171–180.
25 G. M. Spinks, V. Mottaghitalab, M. Bahrami-Samani, P. Whitten and G. G. Wallace, *Adv. Mater.*, 2006, **18**(5), 637–640.
26 N. G. Sahoo, Y. C. Jung, H. J. Yoo and J. W. Cho, *Compos. Sci. Technol.*, 2007, **67**(9), 1920.
27 J. L. Brédas, J. C. Scott, K. Yakushi and G. B. Street, *Phys. Rev. B: Condens. Matter Mater. Phys.*, 1984, **30**(2), 1023.
28 J. Foroughi, S. R. Ghorbani, G. Peleckis, G. M. Spinks, G. G. Wallace, X. L. Wang and S. X. Dou, *J. Appl. Phys.*, 2010, **107**, 103712–103714.
29 Q. Zhang, H. Jin, X. Wang and X. Jing, *Synth. Met.*, 2001, **123**(3), 481–485.

